



OPEN

Driving ferromagnetic resonance frequency of FeCoB/PZN-PT multiferroic heterostructures to Ku-band via two-step climbing: composition gradient sputtering and magnetoelectric coupling

Shandong Li¹, Qian Xue¹, Jenq-Gong Duh², Honglei Du¹, Jie Xu¹, Yong Wan¹, Qiang Li¹ & Yueguang Lü³

¹College of Physics, and Key Laboratory of Photonics Materials and Technology in Universities of Shandong, Laboratory of Fiber Materials and Modern Textile, the Growing Base for State Key Laboratory, Qingdao University, Qingdao 266071, China, ²Department of Materials Science and Engineering, National Tsing Hua University, Hsinchu 30013, Taiwan, ³Department of Physics, School of Science, Harbin Institute of Technology, Harbin 150001, China.

RF/microwave soft magnetic films (SMFs) are key materials for miniaturization and multifunctionalization of monolithic microwave integrated circuits (MMICs) and their components, which demand that the SMFs should have higher self-bias ferromagnetic resonance frequency f_{FMR} , and can be fabricated in an IC compatible process. However, self-biased metallic SMFs working at X-band or higher frequency were rarely reported, even though there are urgent demands. In this paper, we report an IC compatible process with two-step superposition to prepare SMFs, where the FeCoB SMFs were deposited on (011) lead zinc niobate-lead titanate substrates using a composition gradient sputtering method. As a result, a giant magnetic anisotropy field of 1498 Oe, 1–2 orders of magnitude larger than that by conventional magnetic annealing method, and an ultrahigh f_{FMR} of up to 12.96 GHz reaching Ku-band, were obtained at zero magnetic bias field in the as-deposited films. These ultrahigh microwave performances can be attributed to the superposition of two effects: uniaxial stress induced by composition gradient and magnetoelectric coupling. This two-step superposition method paves a way for SMFs to surpass X-band by two-step or multi-step, where a variety of magnetic anisotropy field enhancing methods can be cumulated together to get higher ferromagnetic resonance frequency.

Nowadays integration circuit (IC) technology is developing from system-in-package towards system-on-chip, so the integration of the passive components, such as inductors and capacitors, on one chip is usually adapted in order to miniaturize the electromagnetic devices and to increase the data transmission rate^{1–2}. Microwave soft magnetic films (SMFs) are key materials, which can effectively miniaturize and multifunctionalize the electromagnetic components and devices, such as filters, phase shifters, isolators, circulators, thin film wireless inductors, magnetic recording write heads, antennas, etc.^{3–6}, and reduce their occupation area in MMIC boards. Modern electronic products are heading towards high density, high-frequency, frequency tunability, lightweight and low energy consumption, etc., which give rise to increasing demands for microwave SMFs. Microwave SMFs should have higher ferromagnetic resonance (FMR) frequency (f_{FMR}) and frequency tunability, high permeability, and are to be fabricated in an IC compatible process. In order to reduce the weight and energy consumption of MMICs, researchers are trying to make magnetic devices to be clocked under no magnetic field⁷, i.e. the magnetic properties are manipulated by non-magnetic field methods, such as stress, magnetoelectric coupling, magnetoelastic coupling, etc. instead of bulky and power-consuming electromagnets. Soft magnetic ferrites are not sufficient for MMIC devices due to their lower saturation magnetization ($4\pi M_{\text{S}}$) and permeability, and especially the high fabrication temperature which is incompatible with the IC process⁸. However, metallic soft magnetic films exhibit special advantages in MMIC devices since they have higher $4\pi M_{\text{S}}$ and permeability, and good compatibility with the IC fabrication process. Therefore, self-biased metallic SMFs prepared at IC compatible process have drawn an increasing attention^{9–11}. It was reported that the metallic SMFs are able to operate at

SUBJECT AREAS:
ELECTRONIC DEVICES
ELECTRONIC PROPERTIES AND MATERIALS
MAGNETIC PROPERTIES AND MATERIALS
FERROMAGNETISM

Received
10 September 2014

Accepted
20 November 2014

Published
9 December 2014

Correspondence and requests for materials should be addressed to S.L. (lishd@qdu.edu.cn)



S-band (2–4 GHz) or C-band (4–8 GHz) under self-bias condition^{12,13}. However, to the best of our knowledge, self-biased magnetic films working at Ku-band (12–18 GHz) have not been reported, even though there are urgent needs in achieving tunability in MMICs used in radar, aircraft, satellite, portable communication products, etc.

In this paper, we choose Fe₇₀Co₃₀-B alloys with high $4\pi M_S$ and permeability, and demonstrate a novel method to prepare microwave SMFs at room temperature (an IC compatible process). The novel preparation method combined two magnetic anisotropy fields H_K together (i.e. stress induced H_K by composition gradient and electric field induced tunable H_K via magnetoelectric coupling), realizing a two-step climbing of ferromagnetic resonance frequency. As a result, a giant H_K of 1498 Oe, which is 1–2 orders of magnitude larger than that by conventional magnetic annealing method, and a record high f_{FMR} of up to 12.96 GHz, reaching Ku-band, were obtained at zero magnetic bias field and bias electric field of 8 kVcm⁻¹ in the as-deposited Fe₇₀Co₃₀-B/lead zinc niobate–lead titanate (PZN-PT) (hereinafter referred to as FeCoB/PZN-PT) multiferroic heterostructure films. The ferromagnetic resonance frequency of the FeCoB/PZN-PT multiferroic heterostructures can be manipulated by electric field, instead of large and energy-consuming electromagnets, from 6.30 GHz to 12.96 GHz with the electric field from 0 to 8 kVcm⁻¹. The net frequency shift Δf_{FMR} is as high as 6.66 GHz, and the frequency tunability $\Delta f_{FMR}/f_{FMR}$ is about 106%, equivalent to 832.5 MHz cm kV⁻¹. This electric field manipulation of f_{FMR} shift has low energy consumption and lightweight, especially suitable for manufacturing tuneable MMIC devices.

The ferromagnetic resonance frequency f_{FMR} of SMFs can be expressed by the Kittel equation as follows,

$$f_{FMR} = \frac{\gamma}{2\pi} \sqrt{H_K(H_K + 4\pi M_S)} \quad (1)$$

where γ is the gyromagnetic ratio, $4\pi M_S$ is the saturation magnetization. Clearly, high $4\pi M_S$ and H_K are needed to achieve a high f_{FMR} in SMFs. Previous research on achieving high f_{FMR} SMFs has been mostly focused on enhancing uniaxial magnetic anisotropy field H_K since it is relatively easier to be enhanced by 1–2 orders of magnitude, compared to saturation magnetization that is capped at 24.5 kGs at room temperature^{14,15}. Magnetron sputtering of SMFs in *in-situ* magnetic fields and/or subsequent magnetic annealing after deposition have been widely employed for inducing a uniaxial magnetic anisotropy^{16,17}. However, the induced uniaxial magnetic anisotropy fields are usually in the range of <50 Oe, which leads to limited ferromagnetic resonance frequency of <3 GHz for most of the metallic magnetic films¹⁸.

Several different approaches have been investigated for achieving high uniaxial magnetic anisotropy in SMFs, such as oblique sputtering^{19,20}, facing-target sputtering²¹, exchange coupling^{22–25}, and magnetoelectric coupling^{26,27}, etc. Oblique sputtering and facing-target sputtering can generate magnetic films with H_K of 20–300 Oe^{19,20}. Exchange coupling, such as antiferromagnetic/ferromagnetic exchange coupling^{22–24} and exchange coupling between magnetically soft and hard layers²⁵, provides high H_K around 100–750 Oe. In our previous work, a novel composition gradient sputtering (CGS) method was applied to achieve a high uniaxial magnetic anisotropy in SMFs^{28–30}, which dramatically increased the in-plane uniaxial magnetic anisotropy field to up to 547 Oe due to the uniaxial stress distribution induced by composition gradient. As a result, good microwave ferromagnetic properties with ferromagnetic resonance frequency over 7 GHz were obtained in composition gradient deposited magnetic films.

Multiferroic composite materials have drawn an increased amount of attention recently due to the strong magnetoelectric coupling demonstrated in multiferroic composites, which allows for elec-

tric field manipulation of magnetic properties (converse magnetoelectric effect) or magnetic field control of electric polarization (direct magnetoelectric effect)^{31–34}. The magnetoelectric coupling in magnetic/ferroelectric multiferroic heterostructures can lead to dramatically enhanced electric-field tunable magnetic anisotropy fields approaching 750–880 Oe^{35–37}. Based on the discussion above, it is difficult to obtain SMFs with H_K over 1000 Oe or f_{FMR} over 10 GHz at zero biased magnetic field using a single method. It is necessary to explore novel methods to enhance H_K , and therefore to push the ferromagnetic resonance to X- or Ku-band.

Results

The design for enhancing the ferromagnetic resonance frequency via CGS and magnetoelectric coupling. The FeCoB/PZN-PT multiferroic heterostructures were prepared by a composition gradient sputtering method. The detailed experimental procedures are described as follows: firstly, a (100) single crystal Si substrate with dimension of 75 mm × 5 mm × 0.5 mm was pasted on the turntable with the length direction along the radial (R) direction for optimizing fabrication condition of the CGS SMFs. The sample prepared by CGS method was named as S_{CGS} . The S_{CGS} was cut into 15 segments along the length direction with equal size of 5 mm × 5 mm for microstructure and magnetic properties measurement, and the segments were successively numbered as $n = 1$ to 15 from inner to outer (see the top of Figure 1a inset). Secondly, choose an optimum position (e.g. $n = 13$ in this study), where the comprehensive soft magnetic properties are optimum, then paste a 5 mm × 5 mm (011)-cut PZN-PT single crystal substrate on this optimum position with [100] direction of PZN-PT along the R direction (i.e. [100]//R, see the middle of the Figure 1a inset). The CGS FeCoB film was also deposited on PZN-PT substrate under the same optimum sputtering conditions for studying the electric field manipulation of ferromagnetic resonance via magnetoelectric coupling. So it was named as S_{ME} . Therefore, the effects from composition gradient and magnetoelectric coupling on the microwave soft magnetic properties can be verified by the samples S_{CGS} and S_{ME} , respectively.

Figure 1a shows the schematic drawing of the composition gradient sputtering method. The main target of Fe₇₀Co₃₀ directly faces the centre of the substrate which sits on a rotating turntable, while the doping target of B is offset radially from the sample centre. The doping gun (B target) is tilted at a certain angle towards the sample turntable. This geometrical structure ensures that the materials from the Fe₇₀Co₃₀ main target are distributed homogeneously across the sample, while those from B doping target will have a composition gradient distribution, i.e. B concentration increases gradually from inner to outer positions along the R orientation.

The composition distribution and soft magnetic properties of CGS FeCoB/Si films. The composition distribution along R direction was detected by a field emission electron probe microanalyzer (FE-EPMA). As illustrated in Figure 1b, the atomic ratio between Fe and Co remains at 2.12, indicating a homogeneous composition comparable to the Fe₇₀Co₃₀ target composition; while the B composition y_B increases linearly from 18.07 at.% to 42.12 at.% for the test positions from $n = 1$ to 15, undergoing a linear relation of $y_B = 18.07 + 1.603 * n$ (see Figure 1b). This composition distribution verified the design idea of using composition gradient sputtering to create a composition gradient film with linear doping. The linear doping of B element gives rise to an almost linear increase of H_K and a nonlinear decrease of saturation magnetization $4\pi M_S$. As illustrated in Figure 2, the H_K of CGS FeCoB films increases almost linearly from 90 to 436 Oe, while $4\pi M_S$ rapidly reduces from 14.24 kG ($n = 1$) to 13.21 kG ($n = 5$) at first, then decreases linearly towards 12.72 kG ($n = 15$). The H_K increases nearly 5 times, while $4\pi M_S$ reduces only about 10%, so the ferromagnetic resonance

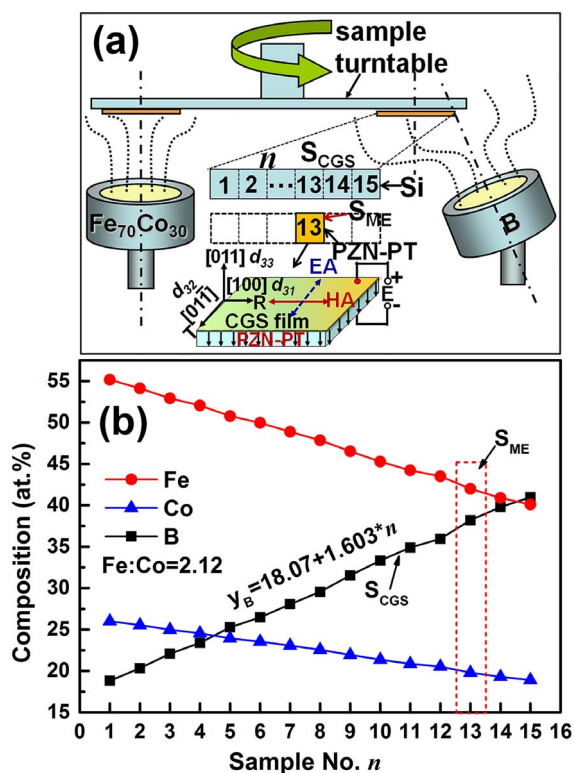


Figure 1 | The CGS device and composition distribution. (a) The schematic drawing of composition gradient sputtering (CGS) device, and (b) the composition distribution detected by a field emission electron probe microanalyzer. The insets of Figure 1a from top to bottom shows the position distribution for CGS sample S_{CGS} and the magnetoelectric coupling sample S_{ME} , and the interaction mechanism of magnetoelectric coupling between CGS film and PZN-PT. The composition distribution of S_{ME} is marked in the inset of Figure 1b using a red short-dashed box.

frequency is dominated by H_K . As expected, the sample position n dependence of f_{FMR} , shown in Figure 3, demonstrates almost the same trend in f_{FMR} with that in H_K (shown in Figure 2). With the increase of n , f_{FMR} increases from 3.18 to 6.73 GHz with increment of 3.55 GHz, equivalent to an increase ratio of 212%. The damping constant α of the CGS FeCoB/Si samples, shown in Figure 3, decreases with the increase of n from 1 to 7, then stays on a low platform with value of 0.011 till $n = 13$, after that α goes up, implying an increase of magnetic loss. Considering the comprehensive magnetic properties including $4\pi M_S$, H_K , f_{FMR} , and α for the segments at different n , we chose $n = 13$ as an optimum position to deposit magnetoelectric coupling sample on PZN-PT substrate since sample $S_{CGS}@n = 13$ shows a relatively large f_{FMR} of 6.45 GHz, large H_K of 402 Oe and low α of 0.0112.

Composition gradient induced uniaxial magnetic anisotropy in CGS films. Some typical hysteresis loops of S_{CGS} are summarized in Figure 4a and 4b. As illustrated in Figure 4a, there is an obvious uniaxial magnetic anisotropy with magnetically easy axis (EA) along tangential direction and magnetically hard axis (HA) along R direction for $S_{CGS}@n = 13$. The n -dependent hysteresis loops along HA are shown in Figure 4b. It can be seen that the H_K increases with the increase of n (or B doping). The detailed H_K variation is shown in Figure 2. The uniaxial magnetic anisotropy in CGS films can be explained as stress gradient induced uniaxial magnetic anisotropy. The intrinsic stress in general is randomly dispersed in the magnetic films which gives rise to a high damping constant and decreasing resonant frequency. However, as reported in our previous work^{28–30}, if a uniaxial stress replaces the randomly

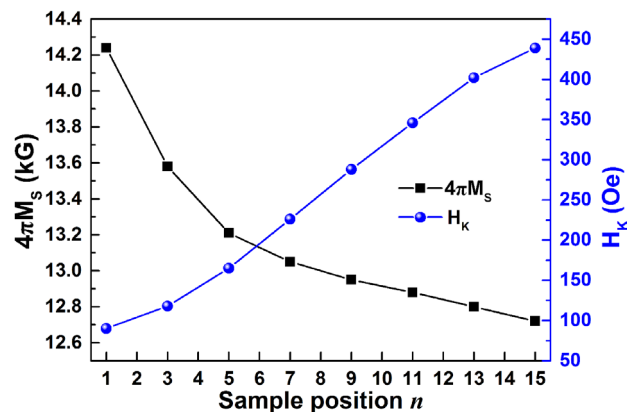


Figure 2 | Sample position n dependence of $4\pi M_S$ and H_K for S_{CGS} .

dispersed intrinsic stress, a stress-induced uniaxial magnetic anisotropy will be obtained. This uniaxial magnetic anisotropy leads to enhanced ferromagnetic resonance and improved microwave magnetic properties. The composition gradient sputtering is an effective way to induce a uniaxial stress, a high uniaxial magnetic anisotropy and an enhanced ferromagnetic resonance frequency.

Combination of stress-mediated CGS and magnetoelectric coupling, and enhancement of microwave soft magnetic properties. As described above, the composition gradient sputtering method gives rise to a compressive stress, leading to a magnetically hard axis along the radial direction. On the other hand, for a (011)-cut PZN-PT single crystal substrate, when the electric field is applied along [011] direction, compressive and tensile stresses will be generated along [100] and [01-1] directions, respectively. According to magnetoelastic energy equation $E_K = -\frac{3}{2}\lambda_S\sigma\cos^2\theta$, for a positive λ_S (as the case in this study for the FeCoB films), a compressive or tensile stress σ will lead to a magnetic anisotropy that forces the magnetic moments to align perpendicular or parallel to the stresses direction, respectively. In other words, the magnetoelectric-coupling-induced magnetic hard axis direction is along [100] direction. So if the [100] direction is parallel to the R direction, the electric-field-tunable effective uniaxial magnetic anisotropy field $(H_K)_{ME}$ will be parallel to the composition-gradient-induced uniaxial magnetic anisotropy field $(H_K)_{CGS}$. Therefore they will be combined together leading to an ultrahigh and tunable uniaxial magnetic anisotropy field H_K (see the bottom of Figure 1a inset). In this study, sample position $n = 13$ was chosen to paste the PZN-PT substrate on, with substrate [100]//R to realize the superposition

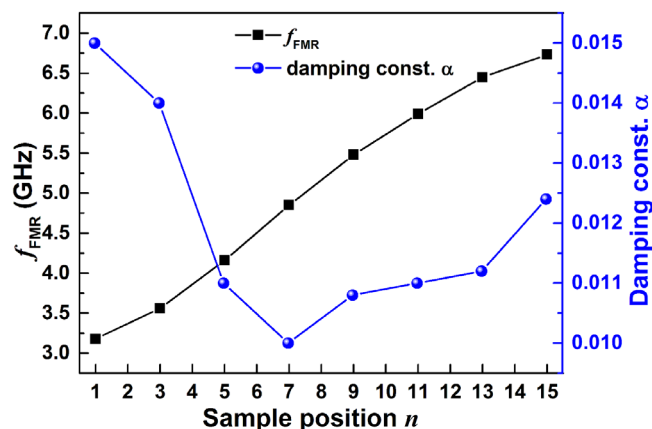


Figure 3 | Sample position n dependence of f_{FMR} and damping constant α for S_{CGS} .

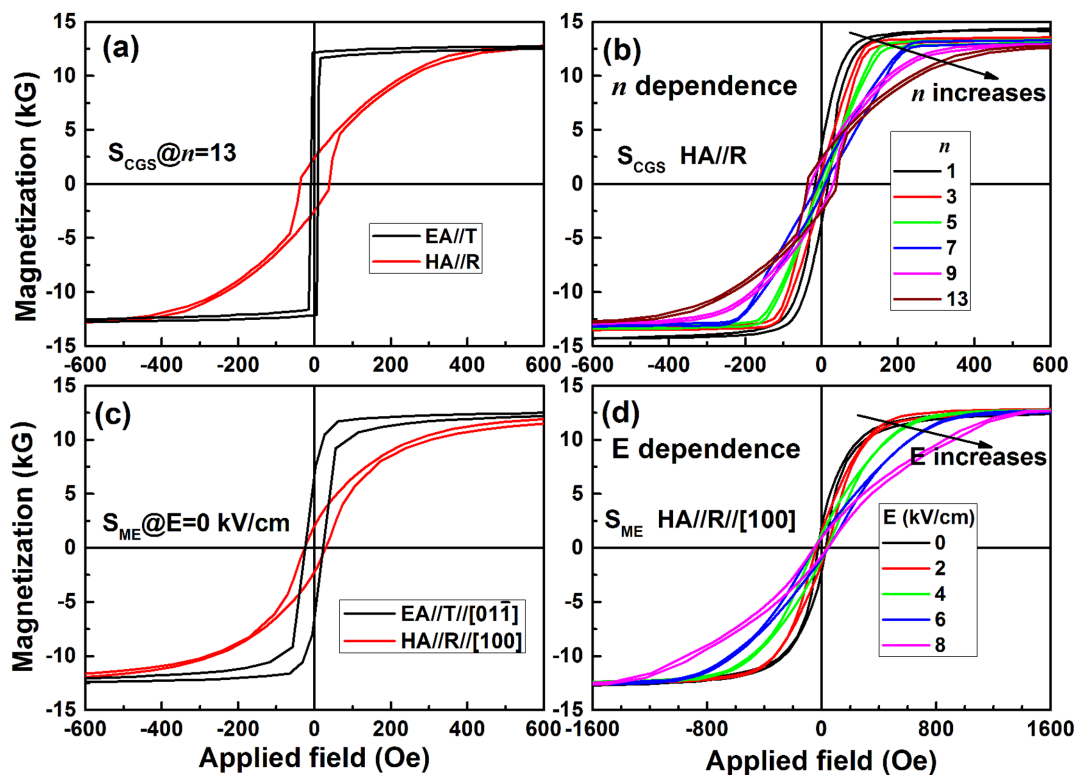


Figure 4 | Sample position and electric field dependent hysteresis loops for S_{CGS} and S_{ME} . (a) Representative hysteresis loops of $S_{CGS}@n = 13$, showing an obvious uniaxial magnetization with HA along R direction; (b) the sample position n dependence of hysteresis loops along HA//R direction for S_{CGS} ; (c) the uniaxial magnetic hysteresis loops of $S_{ME}@E = 0 \text{ kVcm}^{-1}$; (d) the electric field dependence of hysteresis loops of S_{ME} .

of two magnetic anisotropies. As expected, the hysteresis loops of CGS FeCoB/PZN-PT multiferroic heterostructures show a well-defined uniaxial magnetic anisotropy with a H_K of 384 Oe at $E = 0 \text{ kVcm}^{-1}$, slightly smaller than that of 402 Oe on Si substrate (see Figure 4a and 4c). It is exciting that the H_K of S_{ME} dramatically increases with the increase of electric field, and a record high H_K of 1498 Oe was obtained at $E = 8 \text{ kVcm}^{-1}$, implying that an ultrahigh ferromagnetic resonance frequency will be achieved thanks to the combining of composition gradient sputtering and magnetoelectric coupling effect.

Figure 5 shows the frequency dependence of complex permeability for S_{CGS} at various n and for S_{ME} at various electric fields. From Figure 5a, it can be seen that the CGS pushed the f_{FMR} from 3.18 to 6.45 GHz for n from 1 to 13. When the Si substrate was replaced by a PZN-PT substrate, it was found that although the f_{FMR} of 6.30 GHz for $S_{ME}@E = 0 \text{ kVcm}^{-1}$ is slightly smaller than that of $S_{CGS}@n = 13$ due to the difference between the Si and PZN-PT substrates, the magnetoelectric coupling effect dramatically drives the f_{FMR} of FeCoB/PZN-PT multiferroic heterostructures towards 12.92 GHz, directly reaching Ku-band from C-band across X-band. To the best of our knowledge, it is the first report that the ferromagnetic resonance frequency of as-deposited metallic magnetic films can reach Ku-band at zero-bias magnetic field. The magnetoelectric coupling effect in S_{ME} not only generates a 6.66 GHz shift of f_{FMR} under an electric field of 8 kVcm^{-1} , but also provides an electric field tunable ferromagnetic resonance frequency shift over a very broad frequency span, realizing electric field controlled frequency tuning. This is of great significance because it provides the possibility to fabricate electric field tunable microwave devices with large tunability, low energy consumption and light-weight.

The electric field and composition gradient-induced ferromagnetic resonance frequency shift can be explained by the strain/stress-mediated in-plane magnetic anisotropy field. The in-plane ferromagnetic resonance frequency [Equation (1)] can be rewritten as:

$$f_{FMR} = \frac{\gamma}{2\pi} \sqrt{[(H_K)_{CGS} + (H_K)_{ME}] \cdot [(H_K)_{CGS} + (H_K)_{ME} + 4\pi M_S]} \quad (2)$$

where $(H_K)_{CGS}$ is the CGS-induced uniaxial magnetic anisotropic field,

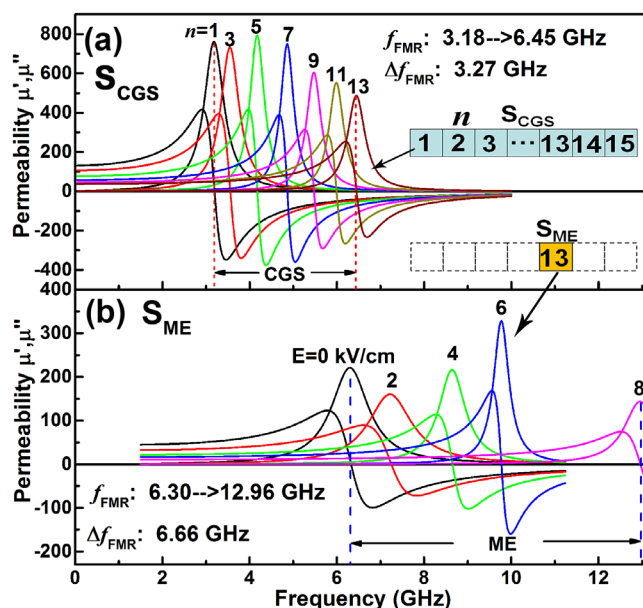


Figure 5 | Frequency dependence of permeability at zero magnetic field for (a) S_{CGS} ($n = 1-13$) and (b) S_{ME} ($E = 0-8 \text{ kVcm}^{-1}$), showing the two-step climbing of f_{FMR} by CGS and ME effects, respectively.



$(H_K)_{ME}$ is the electric-field-induced effective magnetic field which could be positive or negative, and in this study it can be expressed as^{35–37},

$$(H_K)_{ME} = \frac{3\lambda Y}{M_S(1+\nu)}(d_{31} - d_{32})E \quad (3)$$

where Y is the Young's Modulus, ν is Poisson's ratio, λ is the magnetostriction constant of FeCoB film, $d_{31} = -3000 \text{ pC N}^{-1}$ along [100] and $d_{32} = 1100 \text{ pC N}^{-1}$ along [01-1] are linear anisotropic piezoelectric coefficients of PZN-PT, and E is the applied external electric field. $(H_K)_{ME}$ is quantitatively determined by observing the ferromagnetic resonance spectrum shift under various electric fields³⁸. From equation (3), it can be concluded that the $(H_K)_{ME}$ is proportional to the applied electric field due to the magnetoelectric coupling effect, resulting in an electric field tunable f_{FMR} . Similarly, the increase of $(H_K)_{CGS}$ due to the composition gradient will give rise to an upward shift of f_{FMR} .

The sample position n and electric field dependence of magnetic anisotropy field H_K and ferromagnetic resonance frequency f_{FMR} are summarized in Figure 6. As illustrated, the two-step enhancement of H_K and f_{FMR} is clearly observed. Figure 6 is separated into left and right sections by a red dashed line. The left and right sections represent the contributions from composition gradient sputtering and magnetoelectric coupling effect, respectively. In the left section, with the increase of sample position n , the B concentration increases, and the H_K increases linearly from 90 to 402 Oe, leading to an increase of f_{FMR} from 3.18 to 6.45 GHz. In the right section, the CGS FeCoB film was deposited on PZN-PT substrate, and the enhancement effect of electric field on H_K and f_{FMR} begins to function in addition to the CGS effect. So the H_K and f_{FMR} are further pushed up by electric field starting from the corresponding values of S_{CGS} . The H_K and f_{FMR} increase from 384 to 1498 Oe and from 6.30 to 12.96 GHz, respectively, with electric field from 0 to 8 kVcm^{-1} . This two-step superposition method provides a combined effective uniaxial magnetic anisotropy field of up to 1498 Oe at 8 kVcm^{-1} , which is 1–2 orders of magnitude higher than that by the conventional magnetic annealing method. At the same time, the f_{FMR} also directly reaches Ku-band from C-band across X-band.

It is worth mentioning that the strain occurs in the magnetic films due to the composition gradient and the magnetoelectric coupling effect, so a perpendicular anisotropy may arise³⁹. For verifying this issue, the FMR measurement for S_{ME} sample was carried out at various electric fields. In the case of an in-plane applied magnetic field and measuring FMR along the easy axis, the in-plane resonance frequency is well described by Kittel equation, as reported in Ref. 39–41,

$$f_{FMR}^2 = \left(\frac{\gamma}{2\pi}\right)^2 \left[\left(H_r - \frac{2K_{2\parallel}}{M_S} \right) \cdot \left(H_r - \frac{2K_{2\parallel}}{M_S} + 4\pi M_{eff} \right) \right] \quad (4)$$

where $4\pi M_{eff} = 4\pi M_S - \frac{2K_{2\perp}}{M_S}$ defines the effective saturation induction, $\frac{2K_{2\perp}}{M_S}$ is the perpendicular anisotropy field H_{\perp} , and $-\frac{2K_{2\parallel}}{M_S}$ is the in-plane uniaxial anisotropy field H_{eff} ($= (H_K)_{CGS} + (H_K)_{ME}$). The $4\pi M_{eff}$ and H_{eff} can be evaluated by fitting the f vs. H_r plots using equation (4). The fitted H_{eff} is well consistent with the statically measured H_K indicating the experimental data are well fitted using Kittel equation. The FMR fitting results demonstrate that $4\pi M_{eff}$ with an average value of 12.37 kG is slightly smaller than $4\pi M_S$ of 12.79 kG with a small difference of 420 Oe, indicating that a small perpendicular anisotropy may present in the ferromagnetic film. Comparing with the out-of-plane saturation magnetic field of more than 15 kOe, such a small perpendicular field is not enough to drive the magnetic moments to the normal direction of the film. Therefore, the magnetic moments are mainly lying in the plane.

In conclusion, a record high ferromagnetic resonance frequency of 12.92 GHz, which directly reaches Ku-band from C-band across X-band, was obtained in as-deposited CGS FeCoB/PZN-PT multiferroic heterostructures at zero bias magnetic fields due to combining the composition gradient sputtering and magnetoelectric coupling effect together. This two-step superposition method can effectively add two kinds of uniaxial magnetic anisotropy fields together, obtaining ultrahigh H_K that cannot be reached with any single method. This method paves the way to get higher f_{FMR} by two-step or multi-step method. The CGS FeCoB/PZN-PT multiferroic

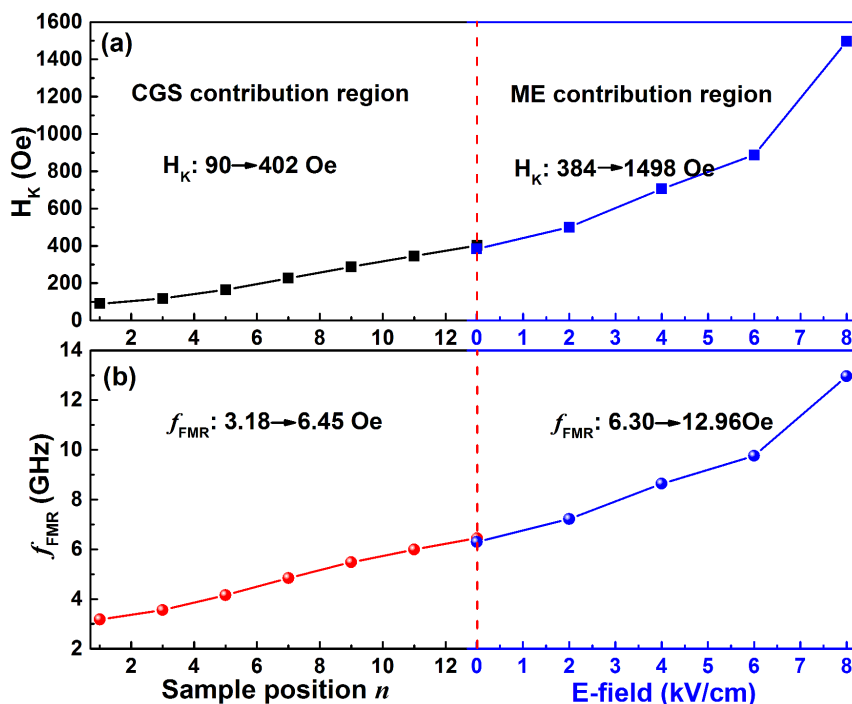


Figure 6 | Sample position n and electric field dependence of (a) H_K and (b) f_{FMR} for S_{CGS} and S_{ME} .



heterostructures exhibit ultrahigh f_{FMR} with very broad electric field tunable frequencies, which provides great opportunities for self-biased voltage tuning microwave multiferroic components working at X-band or higher frequencies without energy consuming electromagnets. All the fabrication processes of the CGS FeCoB/PZN-PT multiferroic heterostructures are carried out at room temperature (i.e. at IC compatible process), which is very beneficial to the integration of these soft magnetic films into monolithic microwave integrated circuits.

Methods

Preparation of the FeCoB/PZN-PT multiferroic heterostructures. The FeCoB films with average thickness of 100-nm were deposited on (100) single crystal Si substrates with dimension of 75 mm \times 5 mm \times 0.5 mm by composition gradient sputtering method at room temperature under 2.8 mTorr Ar atmosphere with a flow rate of 20 sccm, along with a RF power of 80 W for Fe₇₀Co₃₀ target and various powers from 60 to 180 W for B target. The FeCoB films deposited on Si substrate were used to measure magnetic properties, to observe microstructure, and to explore optimum deposition condition. It is found that the sputtering powers of 80 W for Fe₇₀Co₃₀ and 135 W for B target are the optimum deposition condition. Based on the exploring data with Si substrate (as discussed above), the optimum position is at $n = 13$. Afterwards, a (011)-cut single crystal PZN-PT substrate with dimension of 5 mm[100] \times 5 mm[01-1] \times 0.5 mm[011] was pasted at position $n = 13$ (see Figure 1 inset) with [100]//R, and deposited CGS FeCoB film on it under the optimum deposition condition.

Measurement of composition, magnetic, and microwave properties. The composition of films was determined by a FE-EPMA. The magnetic properties were measured by a vibrating sample magnetometer (VSM). The ferromagnetic resonance characteristics of the multiferroic heterostructures were analyzed by a broadband ferromagnetic resonance spectroscopy with the transmission line along the easy axis. The microwave performances were evaluated a vector network analyzer (VNA) with co-planar waveguide. The vector network analyzer acts as a transmitter and a receiver of microwave. The film sample was put on a specially designed co-plane waveguide transmission line fixture. When the microwave passes through the transmission line covered with the soft magnetic film, it will be absorbed by the magnetic film. As a result, the scattering parameter S_{21} will show an absorption peak around the ferromagnetic resonance frequency. The vector network analyzer records the scattering parameters, and simulates the measured curves with LLG (Landau-Lifshitz-Gilbert) equation. Thus, useful parameters such as permeability, ferromagnetic resonance frequency, damping constant, etc. can be obtained.

1. Yamaguchi, M. *et al.* Microfabrication and characteristics of magnetic thin-film inductors in the ultrahigh frequency region. *J. Appl. Phys.* **85**, 7919–7922 (1999).
2. Claasen, T. A. C. M. An industry perspective on current and future state of the art in system-on-chip (SoC) technology. *Proceedings of the IEEE* **94**, 1121–1137 (2006).
3. Sun, N. X. & Srinivasan G. Voltage control of magnetism in multiferroic heterostructures and devices. *SPIN* **02**, 1240004 (2012).
4. Nguyen, C. T. C. Frequency-selective MEMS for miniaturized low-power communication devices. *IEEE Trans. Microwave Theo. Tech.* **47**, 1486–1503 (1999).
5. Luo, Y., Eßeling, M., Zhang, K., Guanterodt, G. & Samwer, K. Magnetoresistance in amorphous oxide films CoFeHfO. *Europhys. Lett.* **73**, 415 (2006).
6. Beach, G. S. D. & Berkowitz, A. E. Co-Fe metal/native-oxide multilayers: A new direction in soft magnetic thin film design II. Microscopic characteristics and interactions (Invited). *IEEE Trans. Magn.* **41**, 2053–2063 (2005).
7. Niemier, M. Magnetic devices: Clocking with no field. *Nature Nanotech.* **9**, 14–15 (2014).
8. Chen, Z. & Harris, V. G. Ferrite film growth on semiconductor substrates towards microwave and millimeter wave integrated circuits. *J. Appl. Phys.* **112**, 081101 (2012).
9. Wang, S. X., Sun, N. X., Yamaguchi, M. & Yabukami, S. Sandwich films: Properties of a new soft magnetic material. *Nature* **407**, 150–151 (2000).
10. Yamaguchi, M. *et al.* Application of bi-directional thin-film micro wire array to RF integrated spiral inductors. *IEEE Trans. Magn.* **36**, 3514–3517 (2000).
11. Chai, G. Z., Phuoc, N. N. & Ong, C. K. Exchange coupling driven omnidirectional rotatable anisotropy in ferrite doped CoFe thin film. *Sci. Rep.* **2**, 832 (2012).
12. Chai, G. Z. *et al.* Adjust the resonance frequency of (Co₉₀Nb₁₀/Ta)_n multilayers from 1.4 to 6.5 GHz by controlling the thickness of Ta interlayers. *Appl. Phys. Lett.* **96**, 012505 (2010).
13. Li, S. D. *et al.* High in-plane magnetic anisotropy and microwave frequency performance of soft magnetic (Fe₅₀Co₅₀)_{1-x}(Al₂O₃)_x films prepared by modified composition gradient sputtering. *IEEE Trans. Magn.* **47**, 3935–3938 (2011).
14. Li, S. D., Yuan, Z. R. & Duh, J. G. High-frequency ferromagnetic properties of as-deposited FeCoZr films with uniaxial magnetic anisotropy. *J. Phys. D: Appl. Phys.* **41**, 055004 (2008).

15. Hashimoto, A., Hirata, K., Matsui, T., Saito, S. & Nakagawa, S. Crystal structure as an origin of high-anisotropy field of FeCoB films with Ru underlayer. *IEEE Trans. Magn.* **44**, 3899–3901 (2008).
16. Shim, J. *et al.* Nanocrystalline Fe-Co-Ni-B thin film with high permeability and high-frequency characteristics. *J. Magn. Magn. Mater.* **290–291**, 205–208 (2005).
17. Jiang, C. J., Xue, D. S., Guo, D. W. & Fan, X. L. Adjustable resonance frequency and linewidth by Zr doping in Co thin films. *J. Appl. Phys.* **106**, 103910 (2009).
18. Seemann, K., Leiste, H. & Bekker, V. Uniaxial anisotropy and high-frequency permeability of novel soft magnetic FeCoTaN and FeCoAlN films field-annealed at CMOS temperatures. *J. Magn. Magn. Mater.* **283**, 310–315 (2004).
19. Li, W. D., Kitakami, O. & Shimada, Y. Study on the in-plane uniaxial anisotropy of high permeability granular films. *J. Appl. Phys.* **83**, 6661 (1998).
20. Yu, E. *et al.* Development of FeCo-based thin films for gigahertz applications. *IEEE Trans. Magn.* **41**, 3259–3261 (2005).
21. Ilijinas, A., Dudonis, J., Bručas, R. & Meškauskas, A. Thin ferromagnetic films deposition by facing target sputtering method. *Nonlinear Analysis Modelling and Control* **10**, 57–64 (2005).
22. Sonehara, M. *et al.* Preparation and characterization of Mn-Ir/Fe-Si exchange-coupled multilayer film with Ru underlayer for high-frequency applications. *IEEE Trans. Magn.* **41**, 3511–3513 (2005).
23. Pettiford, C. *et al.* Effective anisotropy fields and ferromagnetic resonance behaviors of CoFe/PtMn/CoFe trilayers. *IEEE Trans. Magn.* **42**, 2993–2995 (2006).
24. Lamy, Y. & Viala, B. Combination of ultimate magnetization and ultrahigh uniaxial anisotropy in CoFe exchange-coupled multilayers. *J. Appl. Phys.* **97**, 10F910 (2005).
25. Gall, H. L., Youssef, J. B., Vukadinovic, N. & Ostorero, J. Dynamics over 4 GHz of spring-magnet type NiFe-CoFe bilayers with high permeability. *IEEE Trans. Magn.* **38**, 2526–2528 (2002).
26. Fetisov, Y. K. & Srinivasan, G. Electric field tuning characteristics of a ferrite-piezoelectric microwave resonator. *Appl. Phys. Lett.* **88**, 143503 (2006).
27. Srinivasan, G., Zavislyak, I. V. & Tatarenko, A. S. Millimeter-wave magnetoelectric effects in bilayers of barium hexaferrite and lead zirconate titanate. *Appl. Phys. Lett.* **89**, 152508 (2006).
28. Li, S. D., Huang, Z. G., Duh, J. G. & Yamaguchi, M. Ultrahigh-frequency ferromagnetic properties of FeCoHf films deposited by gradient sputtering. *Appl. Phys. Lett.* **92**, 092501 (2008).
29. Li, S. D. *et al.* Microwave frequency performance and high magnetic anisotropy of Fe₇₀Co₃₀-B films prepared by a modified composition gradient sputtering. *IEEE Trans. Magn.* **48**, 4313–4316 (2012).
30. Li, S. D. *et al.* Stress competition and vortex magnetic anisotropy in FeCoAlO high-frequency soft magnetic films with gradient Al-O contents. *J. Appl. Phys.* **113**, 17A332 (2013).
31. Spaldin, N. & Fiebig, M. The renaissance of magnetoelectric multiferroics. *Science* **309**, 391–392 (2005).
32. Eerenstein, W., Mathur, N. D. & Scott, J. F. Multiferroic and magnetoelectric materials. *Nature* **442**, 759–765 (2006).
33. Scott, J. F. Data storage: Multiferroic memories. *Nature Mater.* **6**, 256–257 (2007).
34. Vaz, C. A. F., Hoffman, J., Anh, C. H. & Ramesh, R. Magnetoelectric coupling effects in multiferroic complex oxide composite structures. *Adv. Mater.* **22**, 2900–2918 (2010).
35. Lou, J., Liu, M., Reed, D., Ren, Y. & Sun, N. X. Giant electric field tuning of magnetism in novel multiferroic FeGaB/Lead Zinc Niobate Lead Titanate heterostructures. *Adv. Mater.* **21**, 4711–4715 (2009).
36. Liu, M. *et al.* Giant electric field tuning of magnetic properties in multiferroic ferrite/ferroelectric heterostructures. *Adv. Funct. Mater.* **19**, 1826–1831 (2009).
37. Liu, M. *et al.* Voltage tuning of ferromagnetic resonance with bistable magnetization switching in energy-efficient magnetoelectric composites. *Adv. Mater.* **25**, 1435–1439 (2013).
38. Liu, M. *et al.* Electric field modulation of magnetoresistance in multiferroic heterostructures for ultralow power electronics. *Appl. Phys. Lett.* **98**, 222509 (2011).
39. Belmuguenai, M. *et al.* Temperature dependence of magnetic properties of La_{0.7}Sr_{0.3}MnO₃/SrTiO₃ thin films on silicon substrates. *Phys. Rev. B* **81**, 054410 (2010).
40. Lenz, K. *et al.* Magnetic properties of Fe₃Si/GaAs(001) hybrid structures. *Phys. Rev. B* **72**, 144411 (2005).
41. Nan, T. X. *et al.* Quantification of strain and charge co-mediated magnetoelectric coupling on ultra-thin permalloy/PMN-PT interface. *Sci. Rep.* **4**, 3688 (2014).

Acknowledgments

This work was financially supported by National Natural Science Foundation of China with grant No. 11074040, and Key Project of Natural Science Foundation of Shandong Province with grant No. ZR2012FZ006.

Author contributions

S.L. contributed to the conception, design of the experiment, and writing the manuscript with assistance of J.D. J.D. measured the composition of the samples. Q.X. and H.D.



prepared the samples. J.X., Y.W. and Q.L. measured the microwave and magnetic properties. Y.L. analyzed the data. All authors discussed and commented on the manuscript.

Additional information

Competing financial interests: The authors declare no competing financial interests.

How to cite this article: Li, S. *et al.* Driving ferromagnetic resonance frequency of FeCoB/PZN-PT multiferroic heterostructures to Ku-band via two-step climbing: composition

gradient sputtering and magnetoelectric coupling. *Sci. Rep.* 4, 7393; DOI:10.1038/srep07393 (2014).



This work is licensed under a Creative Commons Attribution 4.0 International License. The images or other third party material in this article are included in the article's Creative Commons license, unless indicated otherwise in the credit line; if the material is not included under the Creative Commons license, users will need to obtain permission from the license holder in order to reproduce the material. To view a copy of this license, visit <http://creativecommons.org/licenses/by/4.0/>